European Conference on Optical Communication (ECOC) 2022 © Optica Publishing Group 2022

Simplified Phase Retrieval Receiver Employing Transmission Fiber for Alternative Projection

Hanzi Huang[(1,2)], Haoshuo Chen[(1,*)], Nicolas K. Fontaine[(1)], Yingxiong Song[(2)], Mikael Mazur[(1)], Lauren Dallachiesa[(1)], Dora Van Veen[(1)], Vincent Houtsma[(1)], Roland Ryf[(1)], and David T. Neilson[(1)]

[(1)] Nokia Bell Labs, 600 Mountain Ave, Murray Hill, NJ 07974, USA, *haoshuo.chen@nokia-bell-labs.com
[(2)] Key Laboratory of Specialty Fiber Optics and Optical Access Networks, Joint International Research Laboratory of Specialty Fiber Optics and Advanced Communication, Shanghai Institute for Advanced Communication and Data Science, Shanghai University, 200444 Shanghai, China, herosf@shu.edu.cn

Abstract *We simplify phase retrieval receiver by directly using transmission fiber as an dispersive element. Performance enhancement is achieved by employing constant modulus constraint of 40-Gbaud QPSK and 8-PSK signal after 40-km single-mode fiber transmission. ©2022 The Author(s)*

Introduction

Reconstruction of the full electric field of an optical signal at the receiver (Rx) enables transmission of advanced modulation formats[1], multiple-input multiple-output processing of polarization- and space-division multiplexed signals[2], and digital compensation of linear and nonlinear impairments[3],[4]. A conventional coherent Rx recovers the entire signal field, but requires a costly laser source as the local oscillator (LO) located in the Rx[5],[6]. To eliminate the need for any reference oscillator and enable coherent-like full-field signal reconstruction with intensity-only measurements, phase retrieval (PR) Rx has been proposed and experimentally demonstrated[7]–[9]. PR Rx based on alternative projection[7] can use low-complexity modified Gerchberg-Saxton (GS) algorithms to recover the full complex valued field from intensity-only measurements. Dispersive propagation which converts phase modulation into amplitude modulation is efficient in projection and relating the intensity-only measurements. Simple PR Rx implementation only uses two photodiodes and a dispersive element[7]. By adding a space-time (ST) diversity block, the performance of the PR Rx can approach conventional coherent detection's sensitivity limit[9]. PR Rx has shown promise in passive optical network (PON) as a colorless full-field recovery scheme to extend transmission distance and increase capacity[10].

In this paper, we experimentally demonstrate a simplified ST diversity PR Rx employing transmission fiber for alternative projection, which can eliminate any additional dispersive element at the Rx. Experimental comparisons are performed between the conventional PR (C-PR) Rx[9] and the simplified PR (S-PR) Rx through recovering 40-GBaud QPSK and 8PSK signals after 40-km single mode fiber transmission. Constant modulus constraint (CMC) of the signal is applied during the iterative process of the PR algorithm and significantly improves the performance of S-PR Rx.

PR Rx with constant modulus constraint

Figure 1(a) shows the schematics of the single-polarization C-PR Rx, which contains a dispersive branch and a ST branch. For C-PR, a dispersive element with the dispersion value of β_{PR} is needed to produce intensity waveform I_B. By iteratively propagating the estimated optical field be-

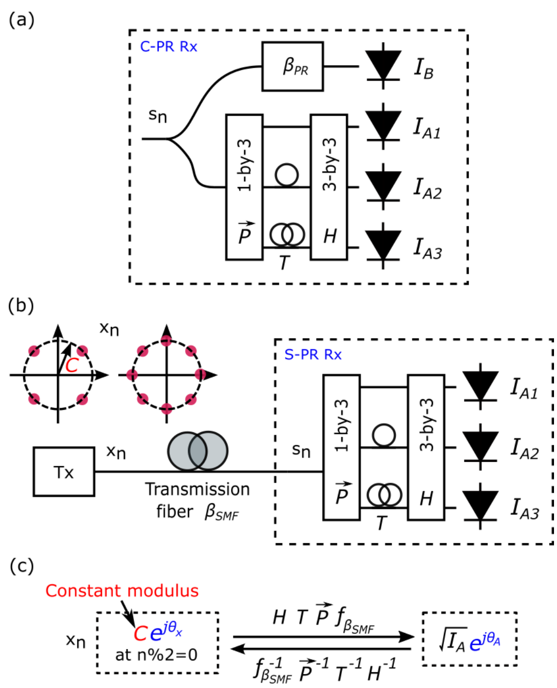

Fig. 1: Schematic diagrams of (a) a conventional PR (C-PR) Rx, (b) a simplified PR (S-PR) Rx to detect constant modulus signals and (c) a modified GS algorithm with CMC for S-PR Rx to iteratively reconstruct the signal.

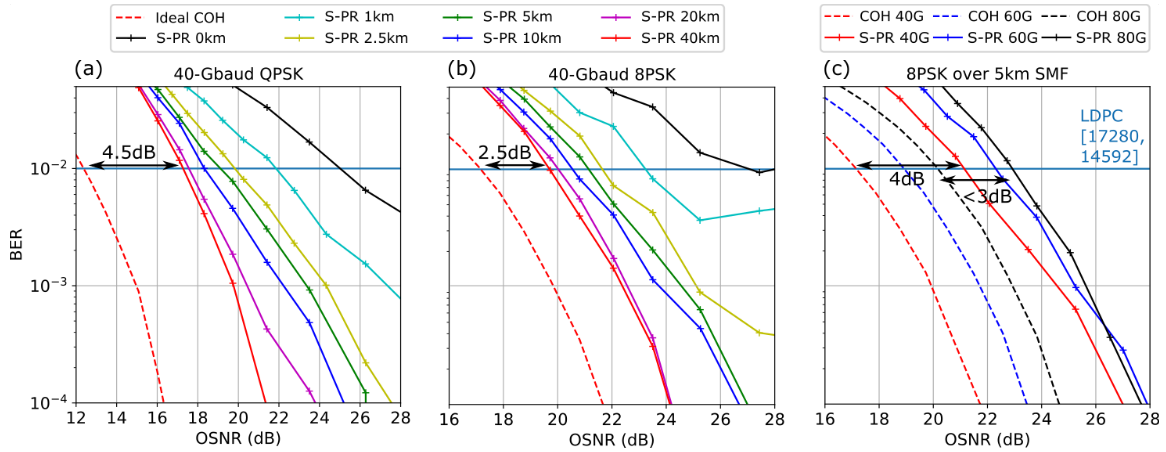

Fig. 2: Simulated BERs versus OSNR for 40-GBaud (a) QPSK, (b) 8PSK signal over various transmission distances and (c) 8PSK signal with different symbol rates over a 5-km SMF transmission.

tween the measured dispersive intensity I_B and spatially mixed intensities I_{An}, the modified GS algorithm is able to retrieve the signal phases.

For constant modulus signals, S-PR directly uses transmission fiber as an alternative dispersive element by employing CMC, which simplifies the receiving structure, as shown in Fig. 1(b). The received complex-valued signal is split equally into three redundant copies each of average power $\vec{P}$, which are then temporally decorrelated by the relative time delay matrix T. The delayed copies are then mixed spatially using a symmetric three-by-three optical coupler with a coupling matrix of H, which equally splits the average power for all the outputs. Three photodiodes (PDs) are used to capture three parallel time-diversity signals with space diversity and generate three intensity measurements at the ST diversity measure plane I_{A1}, I_{A2} and I_{A3}. Fig. 1(c) shows the schematic diagram of S-PR algorithm, where CMCs are applied to each symbol sampling. The estimated phases are updated during the iteration between the two projected planes. To facilitate the convergence of the algorithm, signal bandwidth constraints, pilot symbols and symbol-wise phase reset can be applied[11]. The computational complexity of the modified GS algorithm is $\mathcal{O}(LlogL)$ per iteration due to the FFT operations in computing the dispersion propagation between different projection planes, where L denotes the block length.

Figures 2(a) and (b) plot the simulated BERs of QPSK and 8PSK signals as a function of OSNR at different transmission distances. It can be seen that the performance of a S-PR Rx depends on the link dispersion value, since mixing more symbols benefits the convergence of the algorithm. For a 40-km transmission, a S-PR Rx has small OSNR penalties of 4.5 and 2.5 dB at 10^{-2} forward-error correction (FEC) threshold compared to an ideal coherent receiver for 40-GBaud QPSK and 8PSK formats. Fig. 2(c) shows the simulated BER-OSNR curves of 8PSK over a 5-km single-mode fiber (SMF) transmission, indicating that the OSNR penalty between PR and coherent detection can be further reduced at higher symbol rates for short transmission distances.

Experimental setup

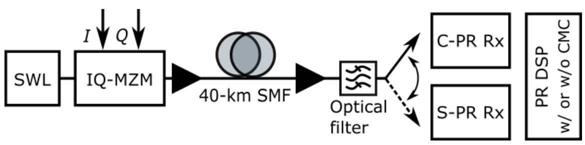

Fig. 3: Experimental setup of characterizing C-PR and S-PR receiving schemes with and without CMC in PR iterations.

Figure 3 shows the experimental setup to characterize the performance of two PR Rx schemes. A swept-wavelength laser (SWL) is used as the light source for modulation to demonstrate the wavelength-independent detection capability of PR Rx[10],[12]. A nyquist-shaped 40-GBaud QPSK signal with a length of 2^{14} is generated from an in-phase and quadrature Mach-Zehnder (IQ-MZM) modulator driven by a two-channel digital-to-analog converter (DAC). An erbium-doped fiber amplifier (EDFA) is used to boost the output power to 11 dBm. After SMF transmission, the received signal is amplified and filtered to eliminate out-of-band noise before being sent to the C-PR and S-PR Rx for comparison. The relative delays of T are 0, 10, 20 symbol periods for both schemes. β_{PR} is set to -330 ps/nm for C-PR. The signal intensities are detected by 40-GHz PIN PDs and captured at 80 GSa/s using a multi-channel analog-to-digital converter (ADC).

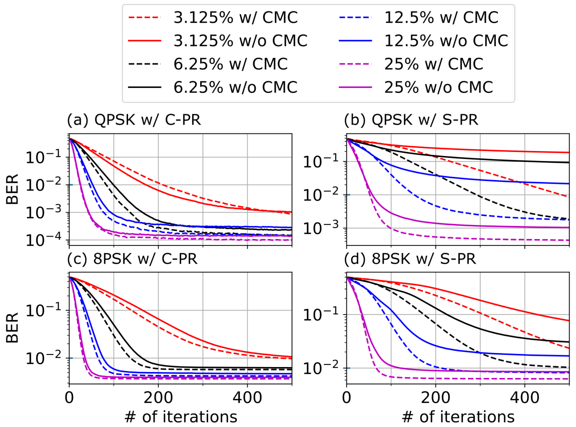

Fig. 4: Measured BER curves versus number of iterations allocating different pilot symbol percentages with and without CMC during iterations for (a) QPSK with C-PR,(b) QPSK with S-PR, (c) 8PSK with C-PR, and (d) 8PSK with S-PR.

The captured waveforms are processed offline. Reconstruction of the signal field is performed by a parallel, block-wise PR algorithm[10] with a block length of 4096 samples at 2 samples per symbol, followed by BER calculation.

Experimental results

Figures 4(a)~(d) show the BERs versus number of iterations for QPSK and 8PSK signals with a C-PR and S-PR Rx employing different pilot symbol percentages, respectively. It can be seen that C-PR generally outperforms S-PR at the cost of hardware and computational complexity. The performance of S-PR is significantly improved by CMC for both modulation formats and for various pilot symbol percentages. Figures 5(a) and (b) show the measured converged BERs of S-PR over time at a wavelength drift rate of 5000-nm/s from 1550 to 1552 nm in a 400-μs time window. Stable BER curves can be achieved for various pilot symbol percentages. With at least 3.125% pilot symbol percentage for the CMC-assisted cases, 7% as well as 20% overhead (OH) FEC thresholds of 4.5×10^{-3} and 2.2×10^{-2} can be achieved for QPSK and 8PSK formats, respectively. The average BERs versus different pilot symbol percentages for QPSK and 8PSK are shown in Fig. 6. For C-PR Rx schemes, the implementation of CMC shows little difference. For S-PR Rx schemes, CMC can reduce the average BERs by 1 to 2 orders of magnitude for a fixed pilot symbol percentage. Assuming a pilot symbol percentage of 3.125%, a net data rate of 72.08 Gbit/s and 93 Gbit/s can be achieved for the S-PR scheme using CMC with a 7% OH FEC using QPSK and a 20% OH FEC using 8PSK format.

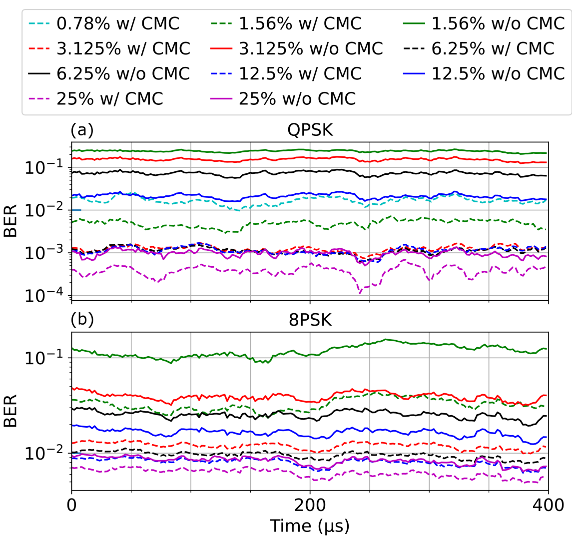

Fig. 5: Measured converged BER curves of S-PR over time corresponding to a wavelength range from 1550 to 1552 nm with different pilot symbol percentages, with and without CMC for (a) QPSK and (b) 8PSK signals.

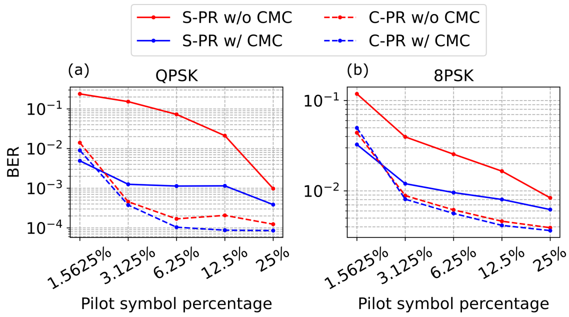

Fig. 6: Average BERs versus different pilot symbol percentages for (a) QPSK and (b) 8PSK for different PR schemes.

Conclusions

We have proposed and experimentally demonstrated a simplified PR Rx directly employing transmission fiber as a dispersive element for alternative projection. For the S-PR Rx scheme, faster convergence, lower percentage of required pilot symbols, and improved BER performance can be achieved using CMC during the algorithm iteration process. While a C-PR Rx generally outperforms its S-PR counterpart in performance, a S-PR Rx with CMC can effectively reduce hardware cost and computational complexity. This work shows that it is possible to eliminate any alternative dispersive element for a PR Rx, thus making a simple, cost-effective Rx front-end to detect carrier-less complex-value signals.

Acknowledgements

This work was supported in part by National Key Research and Development Program of China (2021YFB2900800), the Science and Technology Commission of Shanghai Municipality (20511102400, 20ZR1420900) and 111 project (D20031).

References

[1] F. Buchali, F. Steiner, G. Böcherer, L. Schmalen, P. Schulte, and W. Idler, "Rate adaptation and reach increase by probabilistically shaped 64-QAM: An experimental demonstration", *Journal of Lightwave Technology*, vol. 34, no. 7, pp. 1599–1609, 2016.

[2] J. van Weerdenburg, R. Ryf, J. C. Alvarado-Zacarias, *et al.*, "138-Tb/s mode-and wavelength-multiplexed transmission over six-mode graded-index fiber", *Journal of Lightwave Technology*, vol. 36, no. 6, pp. 1369–1374, 2018.

[3] R. I. Killey, P. M. Watts, V. Mikhailov, M. Glick, and P. Bayvel, "Electronic dispersion compensation by signal predistortion using digital processing and a dual-drive Mach-Zehnder modulator", *IEEE Photonics Technology Letters*, vol. 17, no. 3, pp. 714–716, 2005.

[4] E. Ip and J. M. Kahn, "Compensation of dispersion and nonlinear impairments using digital backpropagation", *Journal of Lightwave Technology*, vol. 26, no. 20, pp. 3416–3425, 2008.

[5] E. Ip, A. P. T. Lau, D. J. Barros, and J. M. Kahn, "Coherent detection in optical fiber systems", *Optics express*, vol. 16, no. 2, pp. 753–791, 2008.

[6] K. Kikuchi, "Fundamentals of coherent optical fiber communications", *Journal of Lightwave Technology*, vol. 34, no. 1, pp. 157–179, 2015.

[7] H. Chen, N. K. Fontaine, J. M. Gene, R. Ryf, D. T. Neilson, and G. Raybon, "Dual polarization full-field signal waveform reconstruction using intensity only measurements for coherent communications", *Journal of Lightwave Technology*, vol. 38, no. 9, pp. 2587–2597, 2020.

[8] Y. Yoshida, T. Umezawa, A. Kanno, and N. Yamamoto, "A Phase-Retrieving Coherent Receiver Based on Two-Dimensional Photodetector Array", *Journal of Lightwave Technology*, vol. 38, no. 1, pp. 90–100, 2020.

[9] H. Chen, N. K. Fontaine, R.-J. Essiambre, *et al.*, "Space-Time Diversity Phase Retrieval Receiver", in *Optical Fiber Communication Conference*, Optical Society of America, 2021, Th4D.3.

[10] H. Chen, N. K. Fontaine, M. Mazur, *et al.*, "140g/70g direct detection pon with $>$37 db power budget and 40-km reach enabled by colorless phase retrieval full field recovery", 2021.

[11] H. Chen, H. Huang, N. K. Fontaine, and R. Ryf, "Phase retrieval with fast convergence employing parallel alternative projections and phase reset for coherent communications", *Optics Letters*, vol. 45, no. 5, pp. 1188–1191, 2020.

[12] H. Huang, H. Chen, N. K. Fontaine, *et al.*, "Experimental characterization of colorless phase retrieval under ultrafast wavelength drift for upstream pon transmission", *Optical Fiber Communication Conference (OFC) 2022*, M4G.5, 2022.